Comparison of Different Spectral Disentangling Techniques Applied to a Triple System

Kelly B. V. Torres[1,2] Luiz Paulo R. Vaz[1] Herman Hensberge[2]

[1]Departamento de Física - ICEx - UFMG - Brazil [2]Royal Observatory of Belgium - Belgium
(kbtorres@fisica.ufmg.br / vaz@fisica.ufmg.br / herman@oma.be)

1. Introduction

Spectral disentangling allows us to reconstruct the contribution of each component of a multiple system to a composite spectrum. In the last decades, algorithms have been developed that operate either on the Fourier components of the spectra or, alternatively, on the velocity bins (logarithm of wavelength). These algorithms are nearly equivalent, except for boundary conditions and applicability of weighting schemes.

We apply both types of technique to a challenging triple system and analyse how far the equivalence goes in practice. We find that the simultaneous use of both types of technique gives insight in the error budget, since each algorithm is in a different way sensitive to particular uncertainties in the input data.

2. The Triple System RV Crt

- RV Crateris (HD 98412; SAO 156604, $V = 9^m$) is an eclipsing triple system of spectral type **F8**.
- The eclipsing close binary (Fig. 1) has an orbital period of 1.17 days.

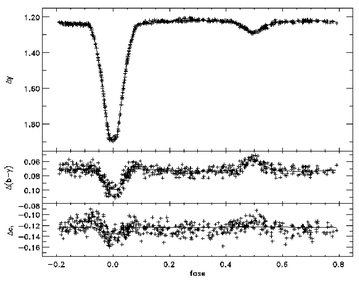

Figure 1. y magnitude differences and Strömgren $b-y$ and c_1 colour index differences between RV Crt and HD 98506 (529 points in each colour) as measured with the Strömgren Automatic Telescope (SAT) at ESO, La Silla, Chile, in 61 nights from 1987 to 1989.

- The distant third component dominates the observed spectrum (Fig. 2)

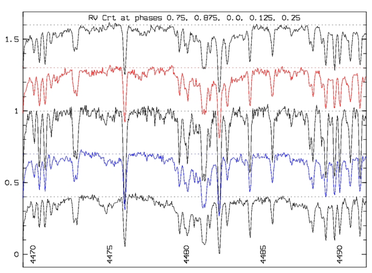

Figure 2. Spectra of RV Crt at different phases. The rotationally broadened lines of the close binary components are hidden by the sharp lines of the the third component. The brighter component of the close binary is best visible as a Doppler-shifting feature near the isolated strong line at λ 4476. The lines of the third component strengthen during the eclipse of the brighter component of the close binary.

We observed RV Crt with the FEROS echelle spectrograph at the MPG/ESO 2.2 m telescope. The high resolution spectra (2.7 $\mathbf{km\,s^{-1}}$) have good signal-to-noise ratio (S/N ≈ 100) over a large wavelength range (λλ 4 200 – 8 800). We used 40 out-of-eclipse spectra and one observed in mid-primary eclipse. Our study shows, in addition to the orbital analysis, that

- The primary and third component are late – F stars, the secondary star is 2 000 K cooler.
- The spectral lines of the primary and the secondary are substantially broadened by rotation, consistent with the rotation being synchronized with the orbital motion.
- The less–massive secondary is larger than the primary.
- The F–star in the close binary is chromospherically active, in contrast to the third component.

3. Saving computing time in Velocity Space

A practical advantage of working in Fourier space is the computational speed. Ill-conditioned equations can also be identified for each mode separately, while a more intricate coupling exists in velocity space. However, masking of blemished data is straightforward in velocity space and the boundary condition to have continuum and the edges of selected wavelength intervals is much less stringent. Therefore, we worked out a scheme to reduce the computational time of the velocity-space based algorithm with minimal loss of accuracy.

The computational time is proportional to the number of bins of the observed spectra, the number of bins in each output component spectrum and the number of observed spectra. It grows fast with the length of the considered spectral region. Dividing the spectral interval in overlapping subregions (Fig. 3) cuts down the computation time significantly. Bins in the output spectra which had at some orbital phase contributions from outside the selected input interval are not used when the subregions are merged. The optimal solution depends in detail on the distribution of the spectra over the orbital phase, but roughly speaking the optimal length of the subregions is of the order of 4 times the amplitude of the largest Doppler shift and less than half of it contributes to the final, merged spectrum. In this way, very large spectral intervals can be processed in a reasonable time.

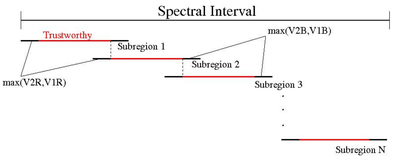

Figure 3. The "spectral interval" is divided in N "subregions" of which the less trustworthy outer parts (black), of length max (V_{2B}, V_{1B}) and max (V_{2R}, V_{1R}), will not contribute to the final output spectra (see text). V refers to the maximal blueward (B) and redward (R) Doppler shifts in the set of input spectra. Note that the "trustworthy" (red) parts of the subregions cover together the whole spectral interval.

4. Different Techniques applied to RV Crt

Originally, we applied the spectral disentangling in the Fourier space using the KOREL code as developed by Hadrava (1995) and adapted to our needs by Vaz (Hensberge et al. 2006). The determination of the orbital parameters involved an iterative process with the analysis of the $uvby$ light curves and the predicted radial velocities. Details about this work can be found in Hensberge et al. (2006). Later, the separation of the spectra was repeated in velocity space using the orbital solution obtained earlier and the code CRES (Ilijić 2004). In this poster, we show (Fig. 4) results for four spectral regions: λλ 4420.41 – 4503.43, 5725.21 – 5832.74, 5828.55 – 5938.02 and 6070.97 – 6184.99. The relative light contribution of the close-binary components varies over this wavelength region from 43% – 41% (primary) and 6.5% – 9.2% (secondary). The third component contributes half of the total light, but due to ellipticity and reflection effects in the close binary, its relative contribution varies slightly over the orbital phase: the tertiary to secondary light ratio varies in our spectra between 5.4 and 6.7.

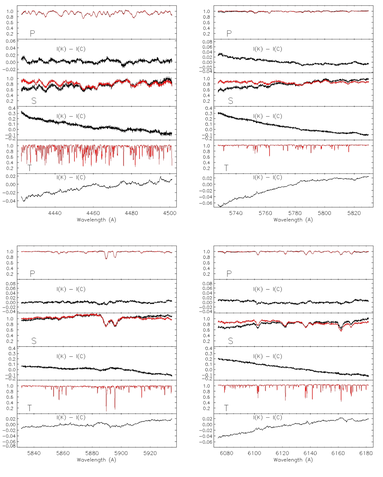

Figure 4. The normalised component spectra (P primary, S secondary, T third component) as obtained by KOREL (red) and CRES (black) and below the difference $\mathrm{I(K)} - \mathrm{I(C)}$ between the solutions.

Spectral separation with the different techniques results in very similar component spectra, with the exception of their low-frequency behaviour. Low-frequency components are easier reconstructed for eclipsed components. Spurious low-frequency components can be removed by much more marginal changes in the normalisation of the input spectra. For the region λλ 6070.97 – 6184.99, Fig. 5 shows the effect of replacing the input spectra $I(p, \phi)$ by

$$\frac{I(p,\phi)}{1 - 0.001 \sin 2\pi\phi \cos 2\pi\frac{p}{2048}} ,$$

where $0 \leq p \leq 2047$ indicates the bin in the spectral interval and ϕ the orbital phase. Note that the amplitudes a of the undulations in the different components are coupled by the relation

$$a_P < \ell_P > + a_S < \ell_S > + a_T < \ell_T >= 0 ,$$

where ℓ indicates the fractional contribution to the total light averaged over all input spectra. In our case, it means that the ratio of the amplitudes of the undulations in the output spectra of the secondary with respect to tertiary are proportional to the ratio $\frac{0.5}{0.092} \approx 5.5$.

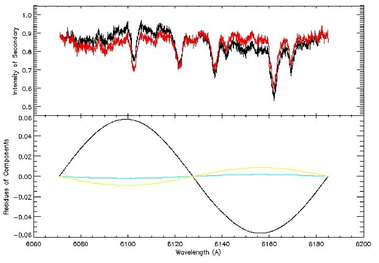

Figure 5. The upper panel: the output spectra of the secondary obtained re-placing the continuum in the input spectra as explained in the text (red) and using the original normalisation (black). The lower panel: changes induced in the output spectra by the continuum replacement in the input spectra, for the primary (blue), secondary (black) and tertiary (yellow).

Both types of technique react in the same way to such re-normalisation. However, this is not the case for all types of biases (Fig. 6). This is a direct consequence of the periodic character of the output spectra induced by the Fourier technique, but not present in the separation in velocity space, as noted already by Ilijić (2004).

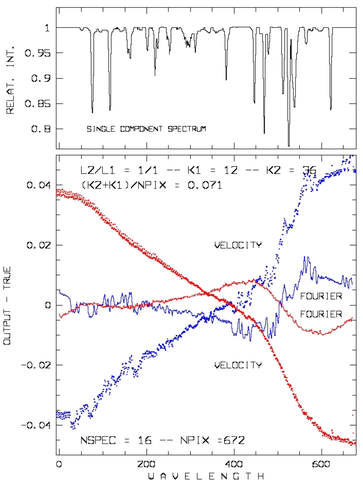

Figure 6. Input spectra (upper panel, single-component spectrum): two identical components with equal luminosity and velocity ratio $\frac{K_2}{K_1} = 3$. The lines of the secondary vary in strength during the orbital cycle: strongly red-shifted lines of that component are stronger by a factor $\frac{4}{3}$, while strongly blue-shifted lines are weaker by a factor $\frac{2}{3}$. The line strength variability, synchronous with the orbit, induces low-frequency bias in both component spectra, but in a much more pronounced way in the separation in velocity space (lower panel).

5. Conclusions

- Fourier and velocity space separation techniques are equivalent in many aspects
- Low-frequency differences in the output spectra obtained by both techniques may contain astrophysically significant information
- Undulations in the output spectra inform about normalisation problems in the input spectra

References

Hadrava, P. 1995, A&AS 114, 393
Hensberge, H., Vaz L.P.R., Torres K.B.V., Armond T. 2006, in: ESO Astrophysics Symposia, Multiple Stars across the HR diagram (eds. S. Hubrig, M. Petr-Gotzens and A. Tokovinin), in press
Ilijić, S. 2004, in: ASP Conf. Ser. Vol. 318, 107

Acknowledgments. We gratefully acknowledge financial support from the Brazilian agency CNPq, the Royal Observatory of Belgium and IAU.